
# Longitudinal changes in human supraspinal processing after RIII-feedback training to improve descending pain inhibition

Philipp Graeff , Ruth Ruscheweyh , Virginia L. Flanagin

PII: S1053-8119(23)00583-9
DOI: https://doi.org/10.1016/j.neuroimage.2023.120432
Reference: YNIMG 120432

To appear in: *NeuroImage*

Received date: 11 December 2022
Revised date: 15 October 2023
Accepted date: 28 October 2023

Please cite this article as: Philipp Graeff , Ruth Ruscheweyh , Virginia L. Flanagin , Longitudinal changes in human supraspinal processing after RIII-feedback training to improve descending pain inhibition, *NeuroImage* (2023), doi: https://doi.org/10.1016/j.neuroimage.2023.120432

# Highlights

- Cognitive strategy learned via RIII feedback training changed haemodynamic activity
- Cognitive strategy application increased activity in pain modulatory areas
- Insula and thalamus are more involved in pain inhibition than previously thought
- Cognitive strategy application decreased haemodynamic response to pain

# Longitudinal changes in human supraspinal processing after RIII-feedback training to improve descending pain inhibition

Philipp Graeff [1,2,], Ruth Ruscheweyh [1,2,3], Virginia L. Flanagin [1,2,4*]

[1] *Research Training Group (RTG) 2175 perception in Context and Its Neural Basis, Ludwig-Maximilians-University Munich, 82152 Planegg, Germany*

[2] *Graduate School of Systemic Neurosciences, Ludwig-Maximilians-University Munich, 82152 Planegg, Germany*

[3] *Department of Neurology, University Hospital Großhadern, Ludwig-Maximilians-University Munich, 81377 Munich, Germany*

[4] *German Center for Vertigo and Balance Disorder (DSGZ), Fraunhoferstr. 20, 82152 Planegg, Germany*

**Corresponding author: vflanagin@lrz.uni-muenchen.de*

**Abstract**

The human body has the ability to influence its sensation of pain by modifying the transfer of nociceptive information at the spinal level. This modulation, known as descending pain inhibition, is known to originate supraspinally and can be activated by a variety of ways including positive mental imagery. However, its exact mechanisms remain unknown. We investigated, using a longitudinal fMRI design, the brain activity leading up and in response to painful electrical stimulation when applying positive mental imagery before and after undergoing a previously established RIII-feedback paradigm. Time course analysis of the time preceding painful stimulation shows increased haemodynamic activity during the application of the strategy in the PFC, ACC, insula, thalamus, and hypothalamus. Time course analysis of the reaction to painful stimulation shows decreased reaction post-training in brainstem and thalamus, as well as the insula and dorsolateral PFC. Our work suggests that feedback training increases activity in areas involved in pain inhibition, while simultaneously decreasing decreases the reaction to painful stimuli in brain areas related to pain processing, which points to an activation of decreased spinal nociception. We further suggest that the insula and the thalamus may play a more important role in pain modulation than previously assumed.

**Keywords:** pain, pain modulation, feedback training, cognitive strategy

1. Introduction

The sensation of pain is a complex process comprising ascending sensory nociception as well as the psychological experience of pain. It can be modulated by endogenous cognitive-emotional processes such as emotions, attention, and beliefs[1–6]. Changes or deficits in endogenous pain modulation are thought to be a driving factor in the chronification of pain, the result of which – chronic pain – is a major global burdens of disease[7,8] .

The ascending pathway for sensory nociception is well known. Nociceptive information enters the central nervous system via the spinal dorsal horn, where it ascends through the brainstem to the thalamus where it disperses within the cortex[9]. There, painful stimuli are processed by the somatosensory cortices, insula, anterior cingulate cortex (ACC), and prefrontal cortex, which provide cognitive and emotional evaluation of the pain[10,1110,12].

In endogenous pain modulation, cortical areas can exert top-down inhibitory control over pain processing[12,13] by targeting pathways descending from the periaqueductal grey (PAG)[13–15] over the rostroventral medulla (RVM)[16,17] and the locus coeruleus (LC)[17,18] to the spinal dorsal horn, where they inhibit nociceptive transmission (at the first synapse). This process is called descending pain inhibition, as it reduces the nociceptive input arriving at the brainstem, and subsequently the reaction of subcortical and cortical regions to painful stimulation.

Patients with chronic pain exhibit impaired descending pain inhibition, a possible reason for pain persistence[8]. Therefore, improving descending pain inhibition in these patients is a promising target for pain therapy[8]. Cognitive-emotional processes such as distraction/attention[2,5,6,19] or positive/negative[20,21] emotions can activate or deactivate descending pain inhibition. We have previously developed a technique that uses positive cognitive emotional training in combination with real-time feedback of the nociceptive flexor (RIII) reflex in response to painful stimulation to improve descending pain inhibition[21]. Patients with chronic pain have successfully used this technique to improve their descending pain inhibition and reduce spinal nociception[22].

Higher cortical regions, such as the lateral[4,23–25] and medial prefrontal cortex[26,27], insula[28,29], and the ACC[25,30,31] are thought to target the origin of the descending pain inhibition pathway[32]. The human literature on cortical modulation of descending pain inhibition, however, has been highly variable[10]. Differences in paradigms and the high degree of individual variability in pain modulation lead to differences in the results[33,34]. Technical constraints make it difficult to determine whether the

reported reduction in pain through cognitive-emotional strategies is truly a result of descending inhibition or rather due to intracortical modulatory processes.

In the present study, we compare brain activity measured with functional magnetic resonance imaging (fMRI) before and after the previously established RIII reflex feedback training paradigm[21]. Subjects learned to use cognitive-emotional strategies to voluntarily activate their descending inhibition under continuous feedback of their spinal nociception as quantified by the spinal RIII (nociceptive flexor) reflex. Quantifying the RIII reflex allows us to ensure that the cognitive strategy employed does indeed reduce spinal nociception, therefore activating descending pain inhibition. We also quantified the RIII reflex to painful stimulation during fMRI. We were interested in how subjects' cognitive strategy affects activity in cortical and subcortical brain regions previously identified to be involved in descending inhibition, and how this strategy influences immediate pain processing in the brain. We expected areas implicated in descending pain modulation to show an increased activity during strategy, which would further increase after RIII feedback training. We additionally hypothesized reduced activity in response to pain during strategy application in pain processing regions, with a further reduction after RIII feedback training.

## 2. Methods

### *2.1. Preregistration*

The desired sample size, variables, hypotheses, and planned analyses were preregistered on the Open Science Framework prior to any data collection under the following link: https://osf.io/gza5n/.

### *2.2. Participants*

This study was conducted in accordance with the Declaration of Helsinki and approved by the ethics committee of the Ludwig-Maximilians-University Munich (19-903). Participants were compensated for their time with 10€/hour. A total of 35 healthy participants were initially recruited via advertisement on the campuses of the Ludwig-Maximilians-University and the University Hospital Großhadern in Munich. Participants had to meet the following criteria for inclusion in the study: (1) age ≥18 years, (2) no severe internal, neurological or psychiatric conditions, (3) no history of chronic pain, (4) no alcohol, nicotine or drug abuse, (5) no regular medication (except hormonal contraception or thyroid hormones), (6) no pregnancy or breastfeeding at the time of participation, (7) no contraindications for MRI scans (incl. but not limited to electrically stimulating implants, medicine pumps, non-MRI-compatible implants or metallic foreign objects in soft tissues). No participants were professional

athletes. Additionally, measurements were postponed if participants had acute pain on the day of, or used pain medication within 48h prior to, the experiment. All participants we briefed on the experimental procedure before giving written, informed consent. Thirty of the initially recruited participants were included in the experiment, four were excluded due to poor RIII reflexes during the introductory session, and one due to an unrelated post-hoc neurological diagnosis (see Section 3.1 for gender and age statistics).

2.3.*Study design*

We were interested in the changes in brain activity after training the voluntary activation of descending pain inhibition. Therefore, we conceptualized a longitudinal experiment where participants' brain activity was measured before and after RIII reflex feedback training. Participants attended a total of 6 sessions, which included an introductory session, the two MRI sessions and three RIII feedback training sessions (Figure 1A). All sessions were conducted on different days, with a minimum of 72h between sessions. The fMRI task was designed to be as similar as possible to the RIII feedback training.

In the introductory session (S0), after giving written informed consent, participants were familiarized with RIII reflex recording. Here we confirmed that a reproducible reflex (>200 µV*ms) could be recorded. We kept the number of painful stimulations to a minimum and did not describe the feedback training to keep participants as naive as possible for the first MRI session. After S0, the first MRI session (MRI1) was performed, in which high resolution anatomical imaging and a RIII reflex functional MRI were performed (see 2.7 fMRI task design). This served as a baseline for all participants before feedback training. Then participants performed the RIII feedback training paradigm we previously established[21,35,36] (S1-S3, described below). Finally, participants' brain activity was measured again in MRI2, with the identical procedure as MRI1.

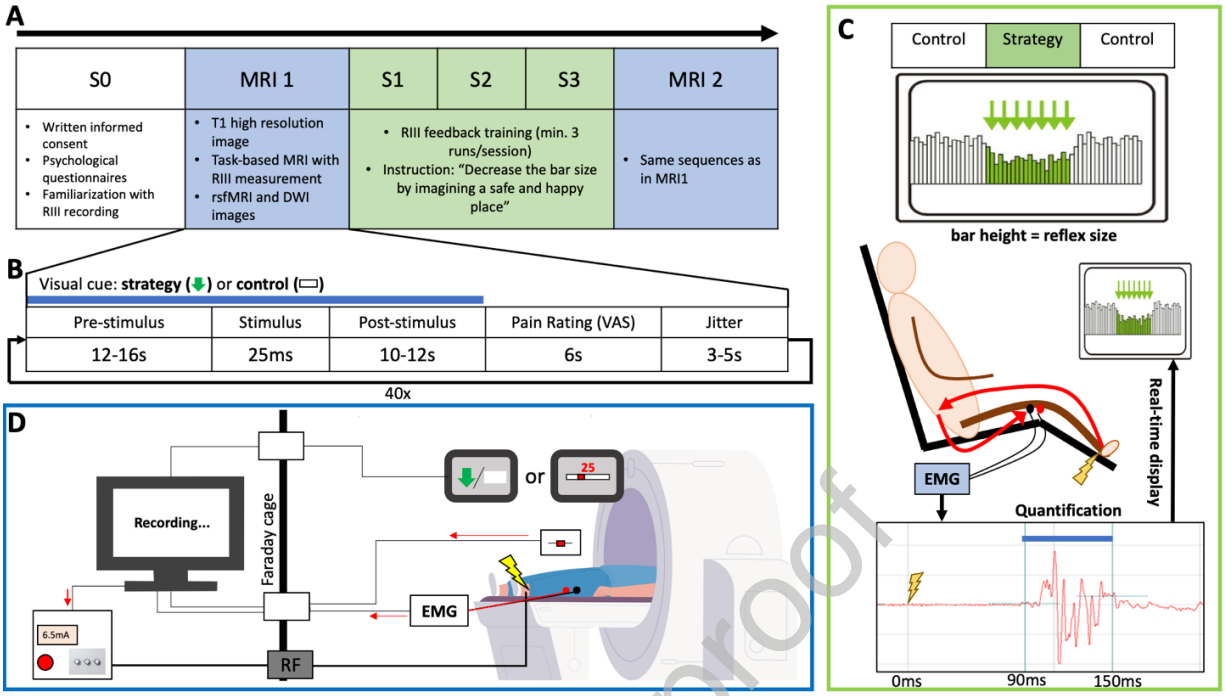


*Figure 1:* ***The entire study design. A The study timeline****. S0 = introductory session, MRI1 = baseline fMRI session, S1-S3 = RIII feedback training, MRI2 = post-training fMRI session.* ***B A single experimental trial in the fMRI experiment (MRI1 & MRI2)****. A single trial lasted between 32 and 40 seconds. Forty trials (20 control, 20 strategy) per experiment were performed, with an average total experiment time of ~26 minutes.* ***C The experimental setup for RIII feedback training sessions (S1-S3)****. Participants received real-time visual feedback of their RIII reflex size and were instructed to apply a positive cognitive strategy during the strategy block* ***D The experimental setup for RIII reflex recording during fMRI (MRI1 & MRI2)****. The computer and stimulator were in the MR control room (outside of the faraday cage). The electrical signal from the stimulator went via the patch panel of the faraday cage and a radiofrequency filter to the stimulation electrode. The EMG signal, VAS signal and visual display signals went to and from the recording computer via waveguides. A single computer ran the experimental script that triggered electrical stimulation, produced visual cues, and simultaneously recorded EMG and VAS responses.*

### *2.4.RIII reflex recording*

To acquire a physiological measure of nociception, we evoked and recorded the RIII reflex as described previously[2,21] and according to established techniques[37,38].

In non-MRI sessions (S0, S1-S3), the participant sat comfortably in a reclining chair with the recorded leg flexed at ~150°. Stimulation and recording were performed with a Keypoint Portable EMG System (Medtonic, Natus, Planegg Germany). Stimulation and recording sites were prepared by degreasing and lightly abrading the skin. Constant current stimulation (5x1ms electrical pulses at 200Hz, 21ms total duration), was applied to the retromalleolar pathway of the sural nerve with a bipolar bar electrode (interelectrode distance 23mm, Natus Europe, Planegg, Germany). RIII reflex responses were recorded from the ipsilateral short head of the biceps femoris using two Ag/AgCl electrodes placed 4-5cm apart. Signals were amplified (up to 10000 times) and band-pass filtered (20-500 Hz), digitized at 24kHz and used for reflex analysis and feedback.

During MRI sessions, the participant lay on the scanner bed with the recorded leg flexed at ~150°. Stimulation and recording sites were located and prepared in the same manner as above. Stimulation (5 x 1ms pulses at 200Hz) was delivered via custom-made MR-compatible electrodes (interelectrode distance, 23mm) and a Digitimer DS7A constant current stimulator (Digitimer Ltd, Welwyn Garden City, UK) triggered by an Arduino UNO microprocessor. The stimulator was equipped with an RF-filter (Mini-Circuits, Camberley, UK) to prevent high frequency interactions in the MRI data. The EMG signal was recorded with an MRI-compatible BrainAmp ExG MR recording system (BrainProducts, Munich, Germany) and digitized at 5kHz. The BrainVision Analyzer MR-correction tool (BrainProducts, Munich, Germany) was used to remove MRI induced artefacts from the EMG trace (baseline correction for average trace, template drift compensation, no downsampling, IIR filter with slope = 48 and cutoff frequency = 150 Hz).

For quantification of RIII reflex areas, EMG signals were rectified, and the area under the curve in the analysis window (90-150ms post-stimulus) was obtained and corrected for average baseline area (30 - 90ms before stimulation).

The stimulation intensity for RIII recording was set at ~150% RIII reflex threshold. The RIII threshold was defined as the stimulus intensity that first evoked a reflex response exceeding a raw area of 100 µV*ms (from the average of 3 series with stimulation intensity increasing from 2.0mA in 0.5mA steps) using a staircase procedure described in more detail elsewhere[2,39]. Average RIII and pain thresholds were 8.3 ± 4.2 mA and 7.1 ± 2.7 mA, respectively.

*2.5.Pain ratings and pain thresholds*

Throughout the entire study, the pain intensity of each electrical stimulation was rated on a numerical rating scale (NRS) from 0 (no pain) to 10 (strongest pain imaginable). The pain threshold was defined as the stimulation intensity that first evoked a NRS rating ≥1 during three ascending series starting from 2mA and increasing in 0.5mA steps. In sessions S0 and S1-3, participants gave verbal pain ratings after each 2 min stimulation block. During MRI sessions, participants rated each stimulus with an MR-compatible sliding scale device.

*2.6.RIII feedback training*

We performed nociceptive RIII reflex feedback training under immediate visual feedback of the RIII reflex size as described previously[21,35,36]. We asked participants to use a positive imagery strategy (i.e. 'Imagine a safe and happy place') to actively decrease their RIII reflex size. During each of 3

feedback sessions, subjects were given the opportunity to optimize their strategy during three to four feedback runs.

A run consisted of 48 consecutively presented painful stimuli every 8-12s, that evoked the RIII reflex. The first 12 stimuli were for reflex stabilization (not analysed). The remaining 36 stimuli were divided into 12 control stimuli (participants were asked not to think of anything in particular), 12 strategy stimuli (participants were asked to use and optimise their strategy to actively decrease the size of their RIII reflexes) followed by another 12 control stimuli (Figure 1C). The strategy block was cued with a green downward arrow appearing on the monitor.

*2.7. fMRI task design*

In the fMRI experiment the strategy or control task was not presented in 2 min blocks of 12 stimuli as in the RIII feedback sessions. Instead single trials with individual visual cues were used to optimize the design for measuring the hemodynamic response function, while remaining as close as possible to the RIII feedback training. In the first MRI session, participants had no information about the cognitive-emotional strategy they would later use for RIII feedback training. Therefore, the instructions regarding the visual cues were simply “Don’t think of anything in particular” during control trials (cue: white bar) or “Imagine a safe and happy place” during strategy trials (cue: green downward arrow). In MRI2, after RIII feedback training, participants were instructed to “Apply the strategy that you developed during the feedback training” during strategy trials. The functional MRI experiment was coded in Matlab (version 2016a, Mathworks) with visual presentation in PsychToolBox3.0 (Version 3.0.11) connected to MR-compatible goggles (NordicNeuroLab, Bergen, Norway).

The experiment was conducted in a single run consisting of 40 trials (20 strategy, 20 control), structured into 8 blocks (4 control, 4 strategy in random order) of 5 trials each. A trial consisted of: cue presentation, a pre-stimulus pseudorandom delay (12-16s), the RIII reflex evoking electrical stimulus, a post-stimulus pseudorandom interval (10-12s), the pain rating (6s) and a jitter (4-6s, Figure 1B). The visual cue was continuously on until the end of the post-stimulus interval, and participants were asked to perform their task (strategy or control) continuously while the cue was present. Pain intensity ratings were captured on a visual 0-100 scale (0= no pain, 100 = strongest pain imaginable) operated by a manual slider.

2.8.RIII reflex and pain rating: statistical analysis

For RIII feedback training sessions, average RIII reflex sizes and pain ratings were calculated separately within all the 12-stimuli control (pre-strategy), strategy, and control (post-strategy) blocks of the respective session and expressed in percent of the control (pre-strategy) average. A repeated measures ANOVA with the factors task (control pre, strategy, control post) and session (S1 and S3) was performed in R (RStudio, version 3.6.3). For MRI sessions, average RIII reflex sizes and pain ratings were calculated over all control or strategy trials of the respective session and again expressed in percent of the control. A repeated measures ANOVA was also performed here with the factors task (strategy, control) and session (MRI1, MRI2). The repeated measures ANOVAs were performed using the lmer() function (lme4[40], version 1.1-26) with significance tested by the Anova() function (car[41], version 3.0-10 ) and post-hoc tests performed using emmeans() (emmeans, version 1.7.2). P-values < 0.05 were considered significant.

Correlations between the RIII reflex and pain reduction in S3 and the change in reflex and pain reduction between the two MRI sessions were calculated using a Pearson correlation in R using the cor.test() function of the stats package.

*2.9.MRI data acquisition*

MRI images were acquired on a 3T Siemens MAGNETOM Prisma scanner (Erlangen, Germany). For each session, a high resolution T1-weighted anatomical image (TR = 2060 ms, TE = 2.17 ms, flip angle = 12 deg., FoV = 240mm , 256 slices, 0.75mm isotropic voxel resolution, A-P phase encoding, GRAPPA = 2), and a field map (TR = 760ms, TE1/TE2 = 4.92ms/7.38ms, dTE = 2.46ms, flip angle = 45 deg., FoV = 240mm, 74 slices, 2.5mm isotropic voxel resolution, A-P Phase encoding) were acquired. Functional images were collected with a 2D multiband EPI sequence with the following parameters: TR = 900ms, TE = 33ms, flip angle = 45 deg., FoV 210mm, 54 slices, 2.5mm isotropic voxel resolution, multiband acceleration factor = 6, A-P phase encoding. The EPI sequence covered the entire brain down to the base of the PONS in all participants. An additional resting state functional and diffusion weighted structural MRI sequence were acquired but not analysed here.

*2.10.* fMRI Preprocessing

Data preprocessing was performed by FMRIPREP version stable[42][RRID:SCR_016216], a Nipype[43] [RRID:SCR_002502] based tool. Each T1w (T1-weighted) volume was corrected for INU (intensity non-uniformity) using N4BiasFieldCorrectionv2.1.0[44] and skull-stripped using antsBrainExtraction.shv2.1.0 (using the OASIS template). Brain surfaces were reconstructed using recon-allfrom FreeSurfer v6.0.1[45]

[RRID:SCR_001847], and the brain mask estimated previously was refined with a custom variation of the method to reconcile ANTs-derived and FreeSurfer-derived segmentations of the cortical gray-matter of Mindboggle[46] [RRID:SCR_002438]. Spatial normalization to the ICBM 152 Nonlinear Asymmetrical template version 2009c[47] [RRID:SCR_008796] was performed through nonlinear registration with the antsRegistrationtool of ANTs v2.1.0[48] [RRID:SCR_004757], using brain-extracted versions of both T1w volume and template. Brain tissue segmentation of cerebrospinal fluid (CSF), white-matter (WM) and gray-matter (GM) was performed on the brain-extracted T1w using fast [49] (FSL v5.0.9, RRID:SCR_002823). Functional data was slice time corrected using 3dTshiftfrom AFNI v16.2.07[50] [RRID:SCR_005927] and motion corrected using mcflirt[51](FSL v5.0.9). This was followed by co-registration to the corresponding T1w using boundary-based registration[52] with six degrees of freedom, using bbregister (FreeSurfer v6.0.1). Motion correcting transformations, BOLD-to-T1w transformation and T1w-to-template (MNI) warp were concatenated and applied in a single step using antsApplyTransforms (ANTs v2.1.0) using Lanczos interpolation. Physiological noise regressors were extracted applying CompCor[53]. Principal components were estimated for the two CompCor variants: temporal (tCompCor) and anatomical (aCompCor). A mask to exclude signal with cortical origin was obtained by eroding the brain mask, ensuring it only contains subcortical structures. Six tCompCor components were then calculated including only the top 5% variable voxels within that subcortical mask. For aCompCor, six components were calculated within the intersection of the subcortical mask and the union of CSF and WM masks calculated in T1w space, after their projection to the native space of each functional run. Frame-wise displacement[54] will be calculated for each functional run using the implementation of Nipype. ICA-based Automatic Removal Of Motion Artifacts (AROMA) was used to generate aggressive noise regressors as well as to create a variant of data that is non-aggressively denoised[55]. As ICA-AROMA already smooths data, we did not perform any additional spatial smoothing. The non-aggressively denoised AROMA images were inclusion-masked using the anatomical brain mask and used as input for first level analysis.

We reduced our preregistered exclusion criteria of a global tSNR of less than 40 in our functional images, as the pilot data was obtained using a much shorter total scanning duration (less than a minute compared to 26 minutes) and tSNR is known to decrease over time[56]. Instead, our mean global tSNR of the raw fMRI images was 35 before preprocessing. After ICA-AROMA correction for movement, we calculated the tSNR for our ROIs and found a mean tSNR of 147 ± 23. We therefore did not exclude any participants based on tSNR (see Supplementary Table 1 for tSNR values of individual ROIs). 3 participants

were excluded due to excessive movement (over ten trials with a framewise displacement (fd)>0.9mm) that was directly associated with the painful stimulus.

*2.11. General linear model analyses*

We were interested in the specific activity in predefined structures known to be involved in pain and descending pain inhibition. However, as additional regions may be involved in the RIII training and altered response to painful stimulation we performed a whole-brain analysis in addition to the ROI analysis. The whole-brain analysis was performed using SPM12 (Version 7771) for Matlab. The single-subject generalized linear model (GLM) included the painful electrical stimulus (**Stimulation**) as an event-predictor of length 0 convolved with the canonical HRF and its first two derivatives. We modelled the derivatives as opposed to the preregistered HRF only, to better account for temporal variation in such a short stimulus. Application of the cognitive strategy or the control was modelled as a boxcar regressor (**Task)** of 2s after the task cue was presented convolved with the canonical HRF, to capture the initial response to task onset. Both stimulation and task were additionally linearly modulated by the relative RIII size and pain intensity on a by-trial basis. These regressors were termed RIII modulated and pain-modulated, respectively. The time the subjects rated their pain via sliding scale was added as a boxcar regressor of no interest. Single volumes in which subjects had a fd>0.9mm were added as nuisance regressors to the model. As ICA-AROMA preprocessing already removed movement related artifacts, we did not add movement parameters as nuisance regressors. Serial autocorrelation of the BOLD time series was modelled with a first-order autoregressive model and low-frequency fluctuations were removed via SPM's DCT with 100s cut-off. Contrasts of interest were constructed for each session by subtracting control from strategy regressors (e.g., $Task_{Strategy}$-$Task_{Control}$) to obtain contrasts for task, stimulation HRF and derivatives, pain modulated task and pain modulated stimulation. The negative contrast (i.e. control – strategy) was created at the group-level analysis.

Group-level analyses were conducted with the Sandwich Estimator (SwE) toolbox[57] for SPM. This toolbox constructs mixed-effects models which takes all random effects into account by using an unstructured covariance structure and as such provides a better estimate of longitudinal and repeated measures data than the classical group-level SPM analysis. We constructed our model with the "classic" SwE type, which estimates the covariance matrix for each subject and session separately, using small sample adjustment type C2. One model per contrast of interest was constructed, inputting the contrasts from MRI1 and MRI2 for each subject. Using non-parametric wild bootstrapping[58] with 5000 permutations and small sample adjustment type C2 with an unrestricted sandwich estimator to

compare contrasts between MRI1 and MRI2. FWE <0.05 was considered significant. Type C2 was used as opposed to Type III (defined in the preregistration) as it was published as the newest recommended correction after writing of the preregistration.

For the ROI analysis, the average beta values for the regressors of interest were extracted from each of the preregistered 16 ROIs (Table 1) for further analysis. We performed four 2x2 repeated measures ANOVAs for each ROI separately using R (RStudio, version 3.6.3). ANOVAs were constructed using the lmer() function of the lme4 package, with condition (strategy/control) and session (MRI1/MRI2) as factors and participant as random effect, using the Anova() function of the car package to test for significance. We further correlated the changes in beta differences (i.e. strategy - control) to changes in pain and RIII reduction between MRI1 and MRI2 as well as the training success, respectively. After Bonferroni correction for multiple comparisons, $p \leq 0.004$ was considered significant for all ROI analyses

All statistical analyses were only performed on the above preregistered regions[59]. However, as alternative definitions of the anterior cingulate subdivisions and dorsolateral prefrontal cortex exist[60,61], an exploratory visualization of the time courses from the ACC, the ventral part of Broadman's area (BA) 8, the BA9 and the dorsal part of BA 46 is also shown. **Error! Reference source not found.** also describes these exploratory regions.

***Table 1: Regions of interest and how they were constructed.*** *Centroids are in MNI coordinates are in MNI space. The lower part of the table included the non-preregistered ROIS and how they were constructed. Centroids from the Brainnetome atlas were calculated from the masks created.*

| **ROI region** | **ROI definition** | **Centroid (mm)** | | |
|---|---|---|---|---|
| | | X | Y | Z |
| Rostroventral Medulla (RVM) | Manual construction of a 40 voxel (1mm isotropic) sheet at z= 49.9mm, covering most of the Medulla | -1 | -39 | -49 |
| Locus coeruleus (LC) | Harvard Ascending Arousal Network[62] | 0 | -38 | -28 |
| Periaqueductal grey (PAG) | Harvard Ascending Arousal Network[62] | 0 | -33 | -12 |
| Anterior congulate cortex (ACC) | FSL Harvard-Oxford Cortical Atlas (threshold = 75) | -1 | 19 | 24 |
| subgenual | 5mm spheres based on coordinates by Zhou et al., 2016[63] | -2 | 24 | -10 |
| perigenual | | -2 | 46 | 10 |
| rostral | | -2 | 34 | 28 |
| Thalamus (R) | FSL Harvard-Oxford Subcortical Atlas (threshold = 75) | 10 | -19 | 7 |
| Thalamus (L) | | -11 | -18 | 7 |
| Hypothalamus | 5mm sphere based on coordinates by Karlsson et al., 2010[64] | 0 | -8 | -8 |
| Insula (R) | FSL MNI Structural Atlas (threshold = 50) | 37 | 4 | -38 |

| | | | | |
|---|---|---|---|---|
| Insula (L) | | -38 | 7 | 2 |
| dlPFC (R) | Combining 'pars opercularis' and 'pars triangularis' from the FSL Harvard-Oxford Cortical Atlas (threshold = 50) | 53 | 20 | 11 |
| dlPFC (L) | | -55 | 21 | 11 |
| mPFC (R) | Combinig 'Rectus' and 'Frontal_Mid_Orb' regions of the AAL3 Atlas[65] | 6 | 43 | -15 |
| mPFC (L) | | -8 | 43 | -14 |
| Non preregistered ROIs (*exploratory analysis*) | | | | |
| Supragenual ACC | 6 mm radius spheres around the approximate coordinates from Meeker et al. (2022)[60] | 0 | 35 | 12 |
| Perigenual ACC | | 0 | 38 | 0 |
| Subgenual ACC | | 0 | 33 | -9 |
| BA8dl (L) | Dorsolateral BA8 from the Brainnetome atlas[66] (threshold 55) | -30 | 23 | 48 |
| BA8dl (R) | | 43 | 26 | 40 |
| BA9l & BA46d (L) | Combined lateral BA9 and dorsal BA46 from the Brainnetome atlas[66] (threshold 55) | -27 | 42 | 31 |
| BA9l & BA46d (R) | | 30 | 37 | 36 |

### *2.12. Timecourse analyses*

We performed a time course analysis on the z-transformed average signal from each ROI, to capture the unknown temporal dynamics which are difficult to assess in a classical general linear model. We were interested in subcortical and brainstem areas with hemodynamics that likely differ from the rest of the brain[67] and with smaller signal-to-noise ratios due to proximity to major blood vessels, CSF flow and breathing artifacts. Because we measured the hemodynamic signal at a temporal resolution of below one second, it is possible to capture additional information about the course of the hemodynamic response function than a general linear model with a fixed impulse response function.

We extracted and z-transformed the raw time courses of our ROIs from the time point of cue-presentation for 12 volumes post-presentation for task and from the time point of stimulation for 12 volumes post-stimulation for stimulation. Z-scores for the analysis of task were then baseline normalized by subtracting the mean value of timepoints 1-4. We analysed the time courses using a repeated measures ANOVA with the factors condition and session while controlling for timepoint in all and side in left/right split ROIs (see Table 1) in R. This gives an impression of the signal change unconstrained by how well the haemodynamics fit the canonical HRF. To account for the delay in haemodynamic response we excluded the first 4 timepoints from the analysis.

In a follow-up analysis we further subdivided the insula ROI into anterior and posterior insula. This was done by splitting the existing ROI mask along is anterior-posterior axis using the central insular sulcus as anatomical landmark.

## 3. Results

*3.1.Participants*

A total of 30 (17 female) participants were included in the study. Mean age was 25 ± 4 years (range: 18-35). 27 of the participants were included in the MRI-analyses (25 ± 4 years, range: 18-35), the three excluded participants had excessive movement (see fMRI preprocessing). The average time between first and second MRI session was 44 ± 23 days (range 14-105).

*3.2.Successful RIII feedback training is indicative of pain reduction during fMRI*

During the three sessions of RIII feedback training, participants used and optimised their personal positive imagery strategy to suppress their RIII reflex while receiving visual feedback on the RIII size. Training success, defined as the reduction in RIII reflex achieved by strategy application during the third training session (S3), was on average to 84 ± 14 % of control (range 57 % to 124 %). This was accompanied by a reduction in pain ratings to 87% ± 10 % of control (range: 55% to 102%). The main effect of task (strategy vs. control) was significant for both RIII reflex area ($F_{2,29}$ = 13.7, p < .001) and pain rating ($F_{2,29}$ = 11.3, p < .001) (Figure 2 A). An interaction between session and task was significant when analysis was limited to those participants who achieved a RIII reduction to at least 90% of control in S3 (n = 22, $F_{2,21}$ = 1.8, p = .027), with an increase in RIII reflex reduction from S1 to S3. There was no interaction for pain ratings ($F_{2,29}$ = 0.1, p = 0.9). Effect sizes (Cohen's d) were 0.51-0.86 for S1-S3 RIII reductions (i.e., in the range of a moderate to large effect according to Cohen) and 1.04-1.41 for S1-S3 pain reductions (large effect).

During fMRI, the RIII reflex size during strategy was reduced to 94 ± 12% of control (range: 71% - 114%) in MRI1 and to 97 ± 13% (range: 75% - 135%) in MRI2. There was a significant main effect of task (strategy vs. control, $F_{1,29}$ = 8.2, p = 0.004) but no significant interaction between task and session ($F_{1,29}$ = 0.637, p = .425) was found. However, the effect sizes were much smaller than in training, MRI1: d = 0.51 MRI2: d = 0.42 (small to moderate effect), respectively, making the null effect problematic to interpret. Pain ratings were also reduced during strategy in both MRI1 (87 ± 19 %, range: 56 % - 135 %) and MRI2 (78 ± 11 %, range: 51 % - 99 %, Figure 2B), with a main effect of task ($F_{1,29}$ = 81.1, p < .001). In contrast to RIII reflex size, pain ratings showed a significant interaction between task and session ($F_{1,29}$ = 5.1, p < .05), i.e., there was a stronger reduction in pain during task in MRI2 compared to MRI1. Effect sizes for pain ratings during task in MRI1 and MRI2 sessions were 0.73 (moderate to large effect) and 1.80 (large effect), respectively.

We designed the study to measure the RIII reflex reduction before and after feedback training during fMRI. However, the measured RIII reflex changes during fMRI were too small draw conclusions

based on the data. Only the increase of pain reduction from MRI1 to MRI2 was significantly correlated with pain reduction in S3 (r = 0.40, p = 0.03, Figure 2C). We were unable to show a direct relationship between the RIII-reflex changes in training and longitudinal changes in the behavioral data collected during MRI data acquisition. Although the RIII reflex training successfully led to a reduced RIII reflex, this did not translate to the MRI sessions. The size of the RIII reflex reductions during MRI were too small to be able to reflect the RIII feedback training success. Reasons for this likely include interference between the participant's position and the RIII reflex measurement, and signal processing constraints related to removing the MRI artifacts from the EMG signal (see discussion for details). Nonetheless, RIII-reflex training, like other behavioral training regimes[68], should lead to changes in neural function that can be measured with fMRI, even without the direct behavioral correlate we had hoped to measure.

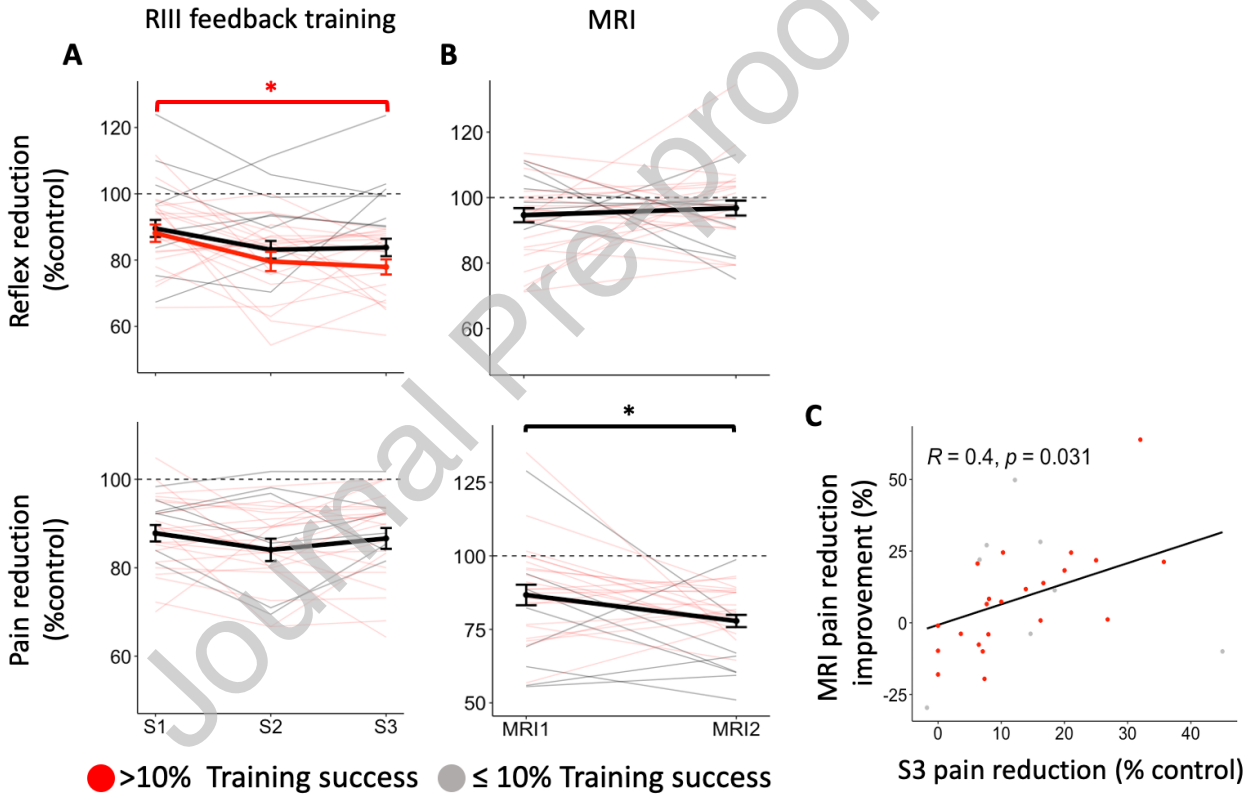


*Figure 2:* ***Behavioural and electrophysiological results****. Individual participants are shown in either grey (unsuccessful training) or pale red (successful training)* ***A) RIII feedback training significantly reduces pain ratings (bottom) and RIII reflex sizes (top).*** *There is a significant main effect of task (p< 0.001), but no interaction between session and condition(black line). The subset of participants that successfully achieved more than 10% RIII reduction in the last session (S3) exhibit significant improvement in RIII reduction between S1 and S3 (p<0.02, red line).* ***B) Pain rating (top) and RIII reflex (bottom) during MRI sessions.*** *Participants showed a significant pain reduction between MRI1 and MRI2 (p= 0.02), but no difference in the RIII reflex. Both MRI1 and MRI2 show a significant reducting in pain rating (p<0.001) during strategy, but no difference was found in individual MRI sessions for the RIII reflex.* ***C) Correlation between pain reduction change in the MRI and pain reduction in the last feedback training session (S3).*** *Individual successful participants (i.e. S3 RIII reflex reduction >10%) are shown in red, participants with <10% reduction shown in grey.*

3.3. *Pain matrix consistently activated by painful electrical stimulation*

Painful electrical stimulation evoked responses in the classical pain matrix, including the insula, S1/S2, ACC, and thalamus (**Error! Reference source not found.** and **Error! Reference source not found.**). The pattern of activity was highly consistent across session and task; no significant differences were found between task and control or between MRI sessions on a whole-brain level when analysed with the GLM.

*3.4.No longitudinal task-specific or pain-specific effects in GLM-based analyses*

Although behavioral differences were evident across training, we found no significant longitudinal differences in brain activity when analysing the data with the GLM. In the whole-brain longitudinal group analysis, we found no significant change between MRI1 and MRI2 in the relative activity during task (i.e., strategy vs. control) or in the relative response to painful stimulation (i.e., strategy vs. control, in all three basis functions). The same was true for the analysis within the predefined ROIs. We also found no correlation between beta values and training success (percent RIII reduction in S3) in the ROI analyses. Furthermore, there was no correlation between the difference in beta values and difference in pain or RIII-reductions between MRI1 and MRI2.

*3.5.Time course analysis revealed both task-specific and pain-specific longitudinal changes within ROIs*

Subtle differences in the timing and strength of the haemodynamic activity within regions is known to be important in pain processing and descending pain modulation and is likely no captured by the GLM. We therefore performed a time course analysis on the mean activity in our regions of interest (see Methods for details).

In the task-specific time course analysis (i.e., the time between cue presentation and painful stimulation), we found significant main effects of task (strategy vs. control) in ACC ($p<0.001$, $F_{1,26} = 36.5$), rACC ($p < 0.004$, $F_{1,26} = 9.8$), sgACC ($p < 0.001$, $F_{1,26} = 15.7$), pgACC ($p < 0.001$, $F_{1,26} = 13.6$), mPFC ($p < 0.001$, $F_{1,26} = 42.5$), dlPFC ($p < 0.001$, $F_{1,26} = 11.8$), and insula ($p < 0.001$, $F_{1,26} = 21.1$). The use of the cognitive strategy increased the hemodynamic activity in all these regions. A significant interaction of task and session was present in hypothalamus ($p < 0.004$, $F_{1,26} = 10.5$), thalamus ($p < 0.004$, $F_{1,26} = 9.5$), dlPFC ($p < 0.004$, $F_{1,26} = 8.6$), and insula ($p < 0.001$, $F_{1,26} = 18.6$). The difference between strategy and control increased from MRI1 to MRI2 in these regions. We observe a similar trend in the PAG, although it was not significant. A significant interaction was also present in the pgACC ($p < 0.004$, $F_{1,26} = 8.8$), but here the difference between strategy and control decreased from MRI1 to MRI2. We additionally found

a significant main effect of side in the dlPFC ($p < 0.0001$, $F_{1,26} = 167.7$), reflected in distinct time courses for each side. Average time courses of those ROIs with significant interactions are plotted in Figure 3. The time courses show a small positive BOLD response after cue onset in most regions (left) and differences between strategy and control are plotted on the right. Supplementary Figure 2A contains the time courses in the ROIs where only a main effect of task is present, and **Error! Reference source not found.** shows four example individual subject time courses.

The follow up analysis in the insular ROI revealed that task related activity was different in anterior and posterior portions. Both anterior ($F_{1,26} = 8.7$, $p < 0.01$) and posterior ($F_{1,26} = 11.2$, $p < 0.001$) insula displayed a strategy-dependant increase in haemodynamic response post training, with the anterior insula displaying a stronger effect. However, only the anterior insula displayed a significant main effect of task ($F_{1,26} = 38.8$, $p < 0.001$) with increased activity during strategy (**Error! Reference source not found.**B).

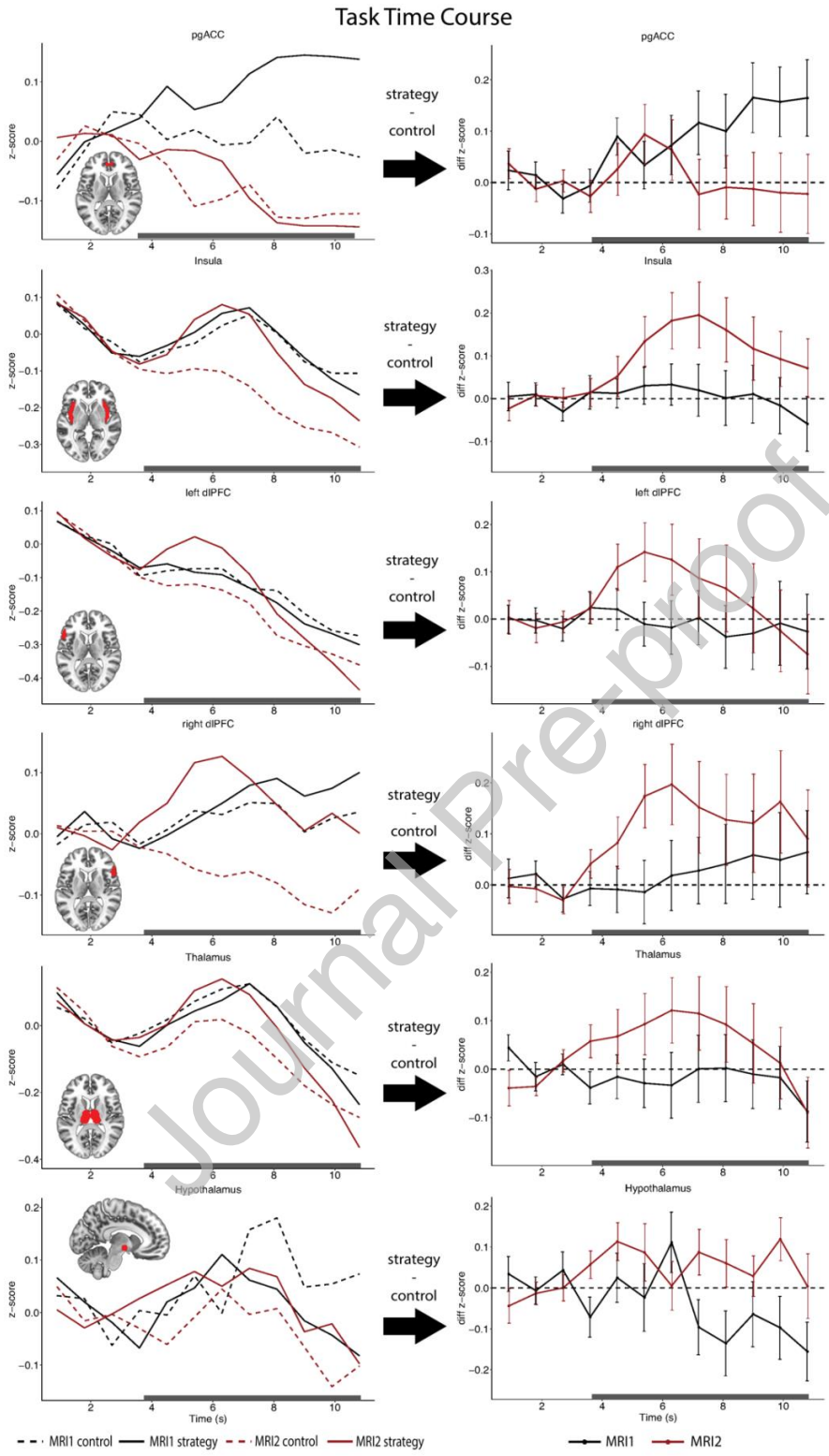


***Figure 3: Z-transformed average MRI signal time courses during the twelve task time points before stimulation.*** *Only those ROIs with a significant interaction between task and session are shown. Left shows the time courses, averaged across trials and participants for the four within-subject conditions that were compared (MRI1 strategy, MRI1 control, MRI2 strategy and MRI2*

*control). Right graphs show the difference between strategy and control for the two MRI sessions. Positive values indicate that the BOLD signal was higher when participants used their cognitive strategy than during control. Participants were instructed to apply the task (control or strategy) for the entire duration shown here. Task cue onset is at t = 0s. Grey bar indicates analysed timepoints. Error bars indicate standard error of the mean. In all significant ROIs, except the pgACC, participants showed a higher BOLD response during strategy in MRI2 than in MRI1 (dlPFC (p < 0.004), Insula (p <0.001), Hypothalamus (p <0.004), Thalamus (p <0.004)). In the pgACC, the difference decreased from MRI1 to MRI2 (p <0.004). Cortical regions are presented first, followed by subcortical regions.*

In the pain-specific time course analysis (i.e., activity in response to the painful stimulation of the sural nerve), we also found significant differences in hemodynamic activity between task and session in our regions of interest. A significant main effect of task was found in rostroventral medulla ($F_{1,26}$ = 11.4, p < .001), locus coeruleus ($F_{1,26}$ = 11.0, p < .001), PAG ($F_{1,26}$ = 11.9, p < .001), and thalamus ($F_{1,26}$ = 23.0 , p < .0001). As hypothesized, the hemodynamic response to the painful stimulus was lower during strategy compared to control. Furthermore a significant interaction between session and task was found in the dlPFC ($F_{1,26}$ = 22.1, p < .0001), insula ($F_{1,26}$ = 10.6, p = .001), thalamus ($F_{1,26}$ = 26.0, p < .0001) and locus coeruleus ($F_{1,26}$ = 12.3 , p<0.001). The relative decrease in signal during strategy was larger in MRI2 compared to MRI1 in these regions. The dlPFC displayed a significant main effect of side ($F_{1,26}$ = 207, p < 0.0001) here as well. The time courses for ROI with significant interactions are plotted in Figure 4. A positive BOLD signal change after stimulation is seen in all conditions and ROIs (left), but the height of the BOLD response significantly changes in these regions (see difference plots on the right). The time courses of the stimulation period were not baseline normalised, as the task-specific time courses were. The differences between time periods appear to develop after stimulation, instead of being present from the start of the time course, which could have been evidence for anticipatory effects[69]. Only in the thalamus are lower strategy-specific BOLD responses present from the start of the time points plotted. Additional time courses of the RVM and PAG can be found in Supplementary Figure 3A and four example individual subject stimulation time courses are seen in Supplementary Figure 5.

We found a significant interaction of session and task in both anterior ($F_{1,26}$ = 4.1, p < 0.05) and posterior insula ($F_{1,26}$ = 5.5, p < 0.05). Haemodynamic response decreased during strategy post-training in both, with the posterior insula exhibiting a stronger decrease (Supplementary Figure 3B). A main effect (i.e., decreased activity during strategy) was present only in the posterior insula ($F_{1,26}$ = 4.8, p < 0.05).

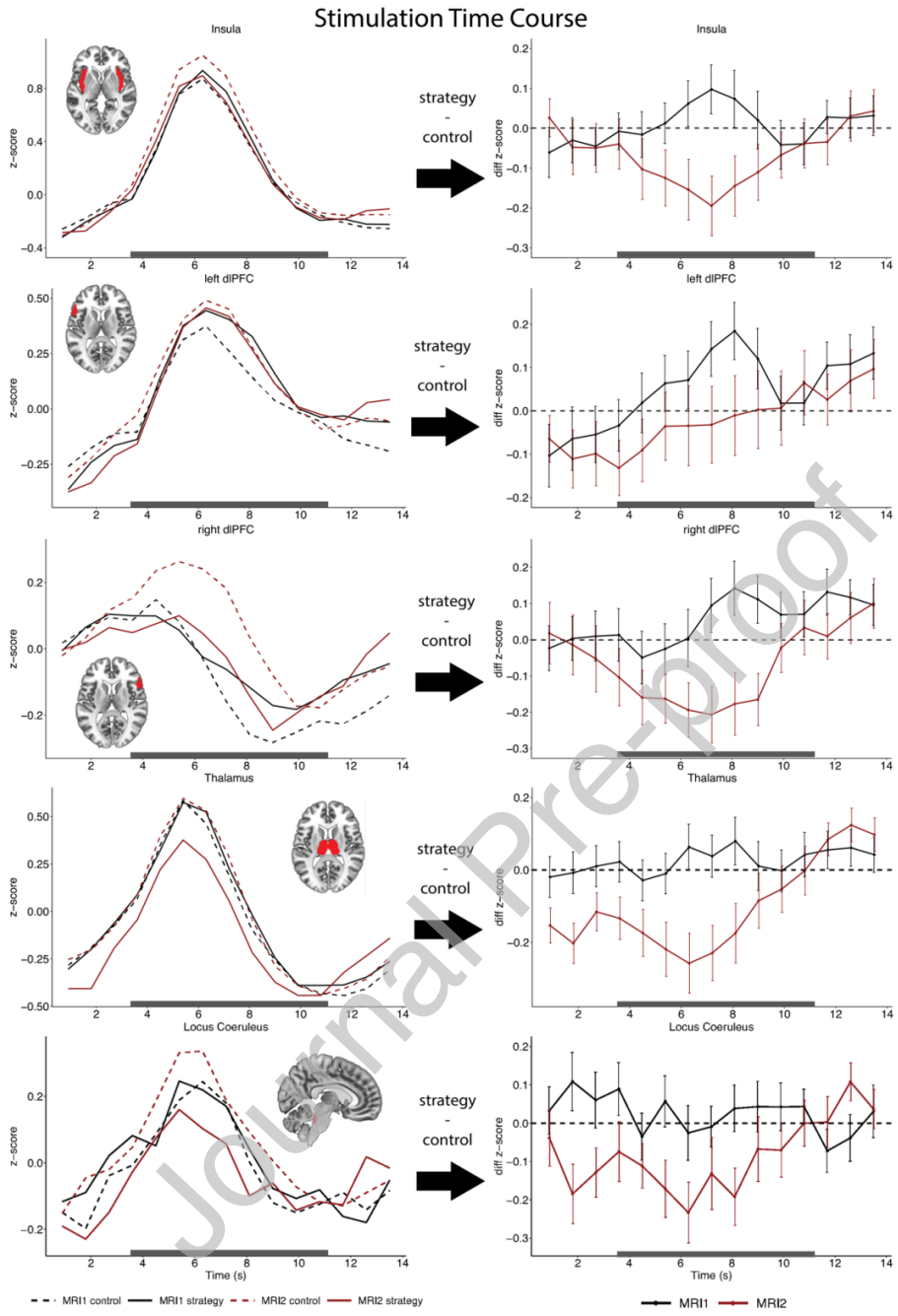


***Figure 4: Time course of z-transformed MRI data after painful stimulation.*** *Only those ROIs with a significant interaction between task and session are shown. Left shows the time courses, averaged across trials and participants for the four within-subject conditions that were compared (MRI1 strategy, MRI1 control, MRI2 strategy and MRI2 control). After painful stimulation, a positive BOLD response is seen in all significant ROIs (see also Supplemental Figure 1). Right graphs show the difference between strategy and control for the two MRI sessions. Negative values indicate that the BOLD signal in response to painful stimulation was lower when participants used their cognitive strategy than during control. Stimulation occurred at t = 0 s. Grey bar indicated the analysed timepoints. Error bars indicate standard error of the mean. During MRI1 the BOLD response to painful stimulation either did not differ between the two task conditions or was slightly higher during the cognitive strategy. After undergoing feedback training, the BOLD signal was significantly smaller in response to painful stimulation during strategy: Locus coeruleus ($p < 0.001$), thalamus ($p < 0.0001$), insula ($p < 0.004$) and dlPFC ($p < 0.0001$).*

There is some debate as to the exact location of some of the pain-specific processing regions that we preregistered for this study. Alternative localisations of the subdivisions of the anterior cingulate exist. The dorsolateral prefrontal cortex is also often defined more dorsal and superior to our definition, encompassing Brodman areas 8, 9 and 46[60,61]. Therefore, as an exploratory visualization, we plotted the time courses of both the task and the stimulation time window for the ACC subdivisions based on [60] and the right and left Broadman areas 8 and a combined BA 9 and 46d in Supplementary Figures 6 and 7. Similar patterns of activity are seen in these ROIs as in our predefined ROIs.

*4. Discussion*

Participants were successful in their ability to reduce their RIII reflex via a cognitive emotional strategy coupled with RIII feedback training, improving their descending pain inhibition to a similar degree as in our previous studies[21,35,36]. Those participants with a lower pain rating at the end of training also showed lower pain ratings while using their learned strategy in the final MRI session, demonstrating the influence of training on pain reduction at a supraspinal level in the absence of feedback. The cognitive emotional strategy affected RIII reflex size in individual participants, an effect that has been found previously[70]. Painful electrical stimulation activated all the cortical and subcortical regions known to be involved in pain processing[71,72].

In a GLM approach, longitudinal differences in brain activity in task-specific strategy use or processing of painful stimulation were not revealed in either a whole-brain or a ROI-based approach. However, longitudinal differences in both strategy- and pain specific activity were seen in a dedicated time course analysis in cortical, subcortical and brainstem regions of interest. The thalamus, insula and dorsolateral prefrontal cortex showed longitudinal and task-related differences in activity both during the cued task period and in response to painful stimulation. Both events led to an increase in BOLD signal in all significant ROIs, although the response to the cue was much smaller than to the painful stimulation. Training led to an increase in BOLD signal while participants use their cognitive behavioral strategy and a relative decrease in BOLD signal in response to painful stimulation.

Pain reduction during strategy use in the MRI was in the expected range, however the concomitant RIII reflex changes were much smaller than previously found behaviorally[21,35,36]. Therefore, the RIII reflex changes obtained during fMRI do not accurately reflect activation of descending inhibitory pathways. Nonetheless, since the decrease in perceived pain during strategy in the MRI, was amplified after training, we maintain that feedback training success translated to the MRI and that this success was related to activation of descending pain inhibition. This is further supported by the significant brain

activity changes found. Individuals can successfully use their strategy for RIII reduction in the absence of RIII feedback even 4 months after training[73].

4.1. Pre-stimulation strategy-related brain activity *intensifies with RIII feedback training*

A time course analysis revealed increases in haemodynamic activity in both cortical and subcortical brain regions when participants use a cognitive emotional strategy to reduce pain. Application of a positive cognitive strategy activated the ACC and PFC, cortical areas related to endogenous analgesia[10,11,74,75], and connected with the PAG[14,76,77]. Application of mental imagery activates descending pathways, even without training[2]. This should be reflected in an overall increase in brain activity and reduction in pain. Indeed, the strategy-related increase in activity in the ACC and mPFC and concomitant experienced pain reduction indicates that these areas activate descending pain inhibition.

Furthermore, the dlPFC, insula, thalamus and hypothalamus become more active during strategy after RIII feedback training. Training also led to an increased suppression of spinal nociception (RIII reflex) and an increased pain suppression after training in both training and MRI session. These results imply that these four regions are sensitive to changes in voluntary activation of descending inhibitory pathways.

The ROIs were chosen for their potential involvement in descending pain inhibition. DlPFC activity has been related to lower perceived pain[24]. Activation of the DlPFC via tDCS exerts an analgesic effect presumably via activation of descending pathways[23,78,79]. The tDCS stimulation of the dlPFC was performed on the left side, supporting the side effects that we found. The additional ROIs we plotted show strongest BOLD signal changes in the combined area BA9 and BA46d, rather than BA8v. The hypothalamus interacts with the PAG[80] and its chemical modulation has a direct relationship to analgesia[81,82].

In contrast, the insula and thalamus are not typically considered cortical players in descending pain inhibition. The insula is thought of as a pain-evaluative and not a modulative region. In our data, the insula, in particular the anterior insula, exhibited the most significant longitudinal increase during strategy application. Stimulation of the insula can elicit antinociceptive effect in both rats[28] and humans[29], suggesting it plays a role in pain modulation as well. Indeed, the anterior insula is active during pain modulation and anticipation[83–85]. The increased BOLD activity during strategy was maintained through the end of the pre-stimulation period, suggestive of attentional or anticipatory

effects[69,86]. However, the activity was no longer different at the start of painful stimulation, and the direction of relative BOLD activity changed during stimulation, less suggestive of anticipatory effects. Similarly, the thalamus' role in pain processing has classically been in relaying the nociceptive signal to higher brain centers, which would not explain the increase in BOLD activity prior to painful stimulation. Valet et al.[6], however, implicated the thalamus in pain inhibition, which would be in line with our data. Unfortunately, the small RIII reflex effect sizes during MRI prevent us from differentiating brain activity related to evaluative, modulative and pain relay effects in our study.

The application of a cognitive strategy may activate more cortical, subcortical and brainstem areas than we observed here. Individual variability in training success may prevent the detection of more subtle subcortical and brainstem effects. Contrary to our results in other cingulo-frontal subregions, the pgACC was the only region to show a relative decrease in activity with training. Perigenual activity has been linked to pain inhibition[6,25], but it has also been suggested to act in anticipation of pain[87,88]. Our results suggest that before training BOLD activity in the pgACC is sustained in the pre-stimulation period, but no longer after training, pointing towards a role of the pgACC in pain anticipation. Brainstem and midbrain regions likely demonstrate smaller effect sizes due to the nature of the fMRI signal in these regions. Nonetheless, the PAG showed a trend towards increased strategy-dependent activity; a good indicator that the pain reduction between MRI1 and MRI2 stems from a stronger activation of descending pain inhibitory circuits.

Our data expand previous results that the ACC, mPFC, dlPFC and hypothalamus are critical for the activation of descending pain inhibition. We suggest that the insula and thalamus may also play a hitherto underestimated role in descending pain modulatory pathways.

*4.2. Lower haemodynamic response to painful stimulation is indicative of reduced nociceptive input*

Pain-specific activity was reduced in areas receiving direct nociceptive input, namely the RVM, PAG and thalamus[9] during the application of the strategy, suggesting that less nociceptive input arrives in the primary recipient structures of ascending pain paths, likely the result of successful descending pain inhibition (Section 4.1). The relative decrease in haemodynamic response after training in the thalamus, and LC in the brainstem, suggests a further reduction in ascending nociceptive input post-training. This may be the result of stronger descending pain inhibition when participants have learned an effective strategy. Interestingly, the lower thalamus activity was present at timepoint 0 of painful stimulation, which suggests anticipatory effects. The thalamus has not classically shown anticipatory

effects to pain, but a meta-analysis revealed that it coactivates with the anterior insula during anticipation of pain[89].

The same longitudinal pattern of lower BOLD activity was reflected cortically in the insula and dlPFC. The insula is one of the primary areas responsible for both the somatosensory and emotional-evaluative experience of pain[10,11]. The larger training effect and strategy-dependent decrease in response to pain in the posterior insula corroborates previous literature implicating it primarily in somatosensory pain processing[90,91]. The role of the dlPFC in pain perception is not fully understood, but it activates in response to acute pain[92,93]. The additional dlPFC ROIs show the strongest BOLD activity in response to painful stimulation in BA9 and BA46d, however the training related effects appear strongest in BA8. The decreased haemodynamic response found in these higher cortical areas after RIII feedback training corresponded to a decreased pain evaluation, which was also found post training.

Lower BOLD responses already within primary receptive areas of ascending pain pathways indicates that nociceptive input is already decreased upon reaching the brain, either via a reduction in the first brainstem relay centers or a decrease in nociceptive transmission on a spinal level. The decreased reaction to the painful stimulation in higher evaluative regions of the brain including the insula and the dlPFC may stem from two mechanisms: either decreased nociceptive input into the brain leads to a proportionately lower reaction in cortical areas, or the cognitive strategy decreases reactivity in these areas, causing a reduced reaction to painful stimuli of the same magnitude. Which mechanism is contributing to the results we see cannot be resolved with this study.

*4.3. A proposal based on imaging descending pain inhibition in humans*

We know from both animal[94–100] and human[101–103] studies the importance of the PAG and brainstem in descending pain modulation. However, the roles of cortical and subcortical regions are less clearly defined. Previous imaging investigations into descending pain modulation have shown the importance of cortical areas such as the ACC and PFC[e.g.4,24,30,31]. However, while descending pain inhibition has been investigated by recording brain activity during painful stimulation, few studies have investigated brain activity during activation of descending pain inhibition independent of painful stimuli. These studies have shown activation of rACC during placebo analgesia[104], of ACC and PFC during conditioning in the CPM paradigm[25] and of the thalamus during distraction mediated analgesia[6].

Our design allowed us to separately investigate both the activity related to activation of descending pain inhibition itself (assessed before application of the painful stimulus) and the effect of

this activation on pain-specific activity in a within-subject design. Activation of descending pain inhibition, achieved with a cognitive strategy, was demonstrated by recording spinal nociceptive activity in the same participants in several cortical and subcortical regions (mPFC, dlPFC, ACC, insula, thalamus, and hypothalamus). During the subsequent response to painful stimulation a set of brainstem, subcortical and cortical regions, who are typically activated during painful stimulation (RVM, LC, PAG, thalamus, insula, and dlPFC), showed a reduced reaction to the painful stimulation. BOLD signal changes were either present during both sessions or enhanced after RIII feedback training.

Our analysis of insular subregions suggests a functional separation between the anterior and posterior insula. It has been previously shown that the anterior insula shown a greater response during modulation[83–85], while the posterior insula serves a somatosensory role[90,91,105]. Functional separation likely exists on an anterior-posterior gradient based on anatomical connectivity[106]. We find task- and pain-specific activity in both areas, with a bias towards the anterior insula for task-related and posterior for pain-related effects. Our findings lend further support to the idea that the anterior insula is preferentially involved in pain modulation, while the posterior insula is active in pain processing. These results suggest that we were able to capture the entire cycle of descending pain inhibition: activation of cortical regions targeting brainstem centers of descending pain inhibition, followed by reduced ascending nociception detected starting in the brainstem. Taking existing knowledge together with our own findings, we propose that feedback training improves the activation of descending pain inhibition in the following way:

Application of the cognitive emotional strategy for descending pain inhibition involves cortical frontal regions, including ACC, PFC and insula. This starts a top-down activation of descending pain inhibition through the thalamus that acts via the brainstem. The dlPFC mediates this activity, through modulation of connectivity between these brain regions, either because of attentional shifts, emotional regulation, or a change in valuation of the stimulus[107–109]. Communication from the cortex to the brainstem most likely originates from two pathways: directly from the PFC and/or ACC, as these areas are connected to the PAG[14,76,110] and the LC, and indirectly through the thalamus, which receives and integrates cortical inputs and can activate descending pain inhibitory processes via its connection to the PAG. When a painful stimulus is then presented, inhibitory signals from the LC and PAG (via the RVM) decrease spinal transmission of nociceptive signals, resulting in decreased nociceptive input into primary receptive regions of both spinothalamic (thalamus) and spinoreticular (RVM and PAG) tracts of pain transmission. This signal propagates to the cortex leading to a reduced response in emotional-evaluative

cortical regions such as the insula and dlPFC, and a resulting decrease in experienced pain. It is possible that the reduced cortical activity is not a bottom-up phenomenon, but a direct result of cortico-cortical interactions. Unfortunately, it is not possible to resolve these two possibilities with the data collected.

The pre-stimulation BOLD activity is likely related to the specific cognitive emotional strategy participants trained instead of a general anticipatory effect. Anticipatory effects have been found in relation to the strength of and waiting time before a painful stimulus[69] both of which did not change in our study. Moreover, the BOLD signal changes were the largest 5-6 seconds after the start of the task cue and in most regions tested normalized to 0 before the start of the painful stimulus, whereas anticipatory signals appear to remain throughout the anticipatory period[69,86]. Positive anticipatory BOLD signal changes are typically associated with an increase in pain rating[86], which we did not find here, with the exception of the dlPFC in placebo analgesia[108]. After training, the thalamus and dlPFC maintain a difference in activity between strategy and control throughout the pre-stimulus time window. In the thalamus, this BOLD activity switched signs; the higher BOLD activity during strategy then dropped below the control condition from the end of the pre-stimulus period through approximately 10 seconds after stimulation. In the right dlPFC, the BOLD activity switched during the stimulation time window and was not maintained after the hemodynamic peak. Based on its role in top-down modulation and regulatory processes as well the structural changes it shows in chronic pain[107], our data support the regulartory role of the dlPFC in pain modulation

Claims about the functional mechanisms or neurotransmitters involved in the effects are challenging to make purely with fMRI and behavioral data. Neurotransmitters affect the fMRI signal in multiple ways: they can directly influence neural activity, the BOLD signal itself, the experienced and physiological pain, and the modulation thereof. Without additional data, it is difficult to determine what neurotransmitters are responsible for the functional and behavioral results we found. Nonetheless, a simultaneous decrease in pain perception and increase in BOLD activity may allow for some insights into possible neurotransmitter mechanisms.

Monoamines including noradrenaline (NA) and serotonin (5-HT) are known to play an important role in descending pain modulation at the level of the midbrain and spinal cord[111]. Opiates are also implicated in pain modulation in the PAG and RVM[112]. In frontal cortical regions, pain modulation is related to glutamate, dopamine and opiate neurotransmitter signaling[113]. The dopamine D2-receptor binding potential increases in prefrontal cortices, including the dlPFC, after therapy and is related to lower anxiety in social anxiety disorder[114]. It also leads to an increase in BOLD activity in frontal areas during a stopping task[115]. The pre- and postsynaptic dopaminergic system appear to be altered in

patients with chronic pain[116], making it an important target system for treatment options. The mu-receptor opiate system has also been implicated in pain modulation[113]. Opioid antagonists block attentional analgesia, a mechanism related to ACC-PAG connectivity[117]. Mu-receptor availability (and not dopamine D2-receptor availability) was negatively correlated with BOLD activity during viewing of painful scenes in the anterior insula thalamus and lateral prefrontal cortex [118]. Rodent models have also shown a reduction in the expression of the mu-receptor in relation to chronic pain behavior[119]. Although this list is far from exhaustive, the location of our results, the BOLD activity and pain perceptual changes found after training and previous work from psychotherapy would suggest that the dopamine D2-receptor and opioid mu-receptor systems are potential players in our RIII-reflex training for descending pain inhibition.

*4.4.Individual variability in descending pain inhibition may impact finding group-level effects*

We expected the longitudinal effects examined here to be robust enough to be identified with a GLM approach. We believe this was not the case due to the variability within our study population. Although positive imagery is the most successful strategy for RIII reflex training on average, not all individuals are successful at using it[21]. Had we allowed participants to use different strategies they may have been more successful pain inhibition, but the brain activity for the task would have been more divergent[33]. The large variability in both training success, as well as in brain activity for any given strategy presents a challenge for obtaining population-level effects with RIII reflex feedback training. The variability in responses across participants is consistent with the pain imaging literature[120,121] and other measures of descending pain inhibition, such as CPM[122,123]. Additionally, imaging research in mindfulness and other mental imagery tasks like the cognitive strategy we used, have typically led to small effect sizes[124–127] making longitudinal comparisons difficult with tractable sample sizes.

Individual training success was a expected source of variability in our study that likely reduces the effect size of the brain activity. Some participants could already reduce their RIII reflex in the first feedback session, suggesting that these individuals, already before training, had a high degree of control over descending pain inhibition using the proposed cognitive strategy. Such a subpopulation of participants strengthens the main effect of cognitive strategy but weakens the longitudinal comparisons we wished to make. Our current study population is too small to stratify into subpopulations and still draw meaningful inferences. In a CPM study, commonly used to assess descending pain inhibition, only a

subgroup of the participants exhibited RIII reflex reductions [70], potentially due to individual differences in the ability to activate the descending pain inhibitory system.

A subpopulation analysis would present an important investigation in descending pain inhibition, particularly for understanding chronic pain patients. A high relative sensitivity to pain and the inability to inhibit pain are seen as potential risk factors for developing chronic pain, across anatomical sites[128]. Chronic pain patients show reduced pain perception after the RIII reflex training but, like healthy controls, not all patients can learn to willfully control descending pain inhibition via RIII reflex training[22]. Future studies will require a better selection of participants or subjects, or a multicenter approach to obtain the larger sample sizes needed to analyse these subpopulations.

*4.5. Improvements and future directions*

The strength of this study was its longitudinal design. By measuring each participant before and after feedback training, we could create a direct, within-subject comparison of brain activity. This is particularly relevant in pain research, as experienced pain is a highly individual and variable phenomenon. We investigated the time preceding the painful stimulus separate from the stimulation event to assess the brain activity when activating descending pain inhibition. Using the RIII feedback training we could physiologically measure the effect the cognitive strategy had on descending pain inhibition. The MRI setup task and design were as congruent with the feedback training as possible. We accounted for potential discrepancies between canonical HRF and the actual haemodynamic response by conducting a time course analysis. This allowed us to detect differences in subcortical and cortical regions where classical analyses often fail.

Nonetheless there are important methodological lessons we can learn here. By constructing a hardware setup for the MRI environment with simultaneous EMG recording and electrical nociceptive stimulation, we were able to read out physiological and psychological measures of nociception/pain. However, measuring the RIII reflex is inherently difficult in an MRI environment. Mutual interference of electrical stimulation, MRI, and electrophysiological recordings added the need for additional safeguards including higher resistance electrodes, on-line filtering of electrical signals, and post-hoc processing with artifact correction. Although the necessary change in body position of the participant between training and MRI sessions may change the RIII-reflex signal, we do not believe this was the case in. our study. Previous work has shown that the perceived pain and the stimulus intensity required to achieve threshold change with body position [129]. Since we adjusted the stimulus intensity to each session individually, and compared pain ratings within session, this should not affect our results. The amplitude

of the RIII reflex does not appear to change with body position[129], therefore the body position should not significantly affect the RIII reflex responses measured. The other methodological changes in the MRI likely prevented us from detecting RIII reflex differences in the MRI. We used a relatively fast EPI sequence with a TR of 900 ms, leading to artifacts with the same frequency as the reflex measured. Although the shape and size of the reflexed recorded were visually indistinguishable to those during training, this overlap in the frequency of signal and artifact could lead to an overall reduction in the variation of the RIII reflex that would explain our low effect sizes. Introducing a short break in each MRI volume acquisition during which painful stimulation can be administered and the EMG reflex recorded[130] could alleviate these effects. The lack of transfer from RIII reflex training success to a RIII reduction during MR imaging prevents us from making the intended direct inferences regarding spinal nociception, however the decreased reaction to stimulation in nociceptive brainstem areas still provide a good indicator of decreased ascending nociceptive input.

*5. Conclusion*

Our investigation revealed that multiple cortical and subcortical structures implicated in descending pain inhibition are activated when employing a positive cognitive-emotional strategy and increase further after training. Complementary thereto, the haemodynamic response to pain in regions receiving initial nociceptive input, as well as cortical-evaluative regions is decreased after employing the learned strategy. Our findings complement the existing body of literature by showing the full timeline of initiating descending pain inhibition to decreased nociception in one study by measuring brain activity of taught activation of descending pain inhibition and its effect on ascending nociception and supraspinal pain processing in the same experiment.



**Data availability statement:** Defaced data in BIDS format will be made publicly available upon acceptance on https://gin.g-node.org/

**Declaration of Interest:** The authors declare no conflict of interest.

**Acknowledgements**. We would like to thank all participants for their participation in the study, Mathias Hübner for his help at the MRI facilities, and Jens Sommer for providing the RIII feedback software. Further thanks goes to Enrico Schulz for the many discussions regarding the MRI setup and data.

Supported by Deutsche Forschungsgemeinschaft (DFG, German Research Foundation) via a grant for major research instrumentation (DFG, INST 409/193-1 FUGG), and the "RTG2175: Perception in context and its Neural Basis", Graduate School of Systemic Neurosciences (GSC 82/1).

References:

1. Rhudy, J. L., Williams, A. E., McCabe, K. M., Nguyên, M. A. T. V. & Rambo, P. Affective modulation of nociception at spinal and supraspinal levels. *Psychophysiology* **42**, 579–587 (2005).
2. Ruscheweyh, R., Kreusch, A., Albers, C., Sommer, J. & Marziniak, M. The effect of distraction strategies on pain perception and the nociceptive flexor reflex (RIII reflex). *Pain* **152**, 2662–2671 (2011).
3. Lee, J. *et al.* Encoding of Self-Referential Pain Catastrophizing in the Posterior Cingulate Cortex in Fibromyalgia. *Arthritis & Rheumatology* **70**, 1308–1318 (2018).
4. Wiech, K. *et al.* Anterolateral prefrontal cortex mediates the analgesic effect of expected and perceived control over pain. *Journal of Neuroscience* **26**, 11501–11509 (2006).
5. Bantick, S. J. *et al.* Imaging how attention modulates pain in humans using functional MRI. *Brain* **125**, 310–319 (2002).
6. Valet, M. *et al.* Distraction modulates connectivity of the cingulo-frontal cortex and the midbrain during pain - An fMRI analysis. *Pain* **109**, 399–408 (2004).
7. Vos, T. *et al.* Global, regional, and national incidence, prevalence, and years lived with disability for 328 diseases and injuries for 195 countries, 1990-2016: A systematic analysis for the Global Burden of Disease Study 2016. *The Lancet* **390**, 1211–1259 (2017).
8. Yarnitsky, D. Role of endogenous pain modulation in chronic pain. *Pain* **156**, 24–31 (2015).
9. Basbaum, A. I., Bautista, D. M., Scherrer, G. & Julius, D. Cellular and Molecular Mechanisms of Pain. *Cell* **139**, 267–284 (2009).
10. Apkarian, A. V., Bushnell, M. C., Treede, R. D. & Zubieta, J. K. Human brain mechanisms of pain perception and regulation in health and disease. *European Journal of Pain* **9**, 463 (2005).
11. Tracey, I. & Mantyh, P. W. The Cerebral Signature for Pain Perception and Its Modulation. *Neuron* **55**, 377–391 (2007).
12. Garcia-Larrea, L. & Peyron, R. Pain matrices and neuropathic pain matrices: A review. *Pain* **154**, (2013).
13. Ossipov, M. H., Dussor, G. O. & Porreca, F. Review series Central modulation of pain. *J Clin Invest* **120**, 3779–3787 (2010).
14. An, X., Bandler, R., Öngür, D. & Price, J. L. Prefrontal cortical projections to longitudinal columns in the midbrain periaqueductal gray in Macaque monkeys. *J Comp Neurol* **401**, 455–479 (1998).
15. Petrovic, P., Kalso, E., Petersson, K. M. & Ingvar, M. Placebo and opioid analgesia - Imaging a shared neuronal network. *Science (1979)* (2002) doi:10.1126/science.1067176.
16. Basbaum, A. I., Ralston, D. D. & Ralston, H. J. Bulbospinal projections in the primate: A light and electron microscopic study of a pain modulating system. *Journal of Comparative Neurology* **250**, 311–323 (1986).
17. Stamford, J. A. Descending control of pain. *Br J Anaesth* **75**, 217–227 (1995).
18. Llorca-Torralba, M., Borges, G., Neto, F., Mico, J. A. & Berrocoso, E. Noradrenergic Locus Coeruleus pathways in pain modulation. *Neuroscience* **338**, 93–113 (2016).
19. Tracey, I. *et al.* Imaging Attentional Modulation of Pain in the Periaqueductal Gray in Humans. *Journal of Neuroscience* **22**, 2748–2752 (2002).
20. Ruscheweyh, R., Albers, C., Kreusch, A., Sommer, J. & Marziniak, M. The effect of catastrophizing self-statements on pain perception and the nociceptive flexor reflex (RIII reflex). *Clinical Journal of Pain* (2013) doi:10.1097/AJP.0b013e318272ec0c.
21. Ruscheweyh, R. *et al.* Learned control over spinal nociception reduces supraspinal nociception as quantified by late somatosensory evoked potentials. *Pain* **156**, 2505–2513 (2015).

22. Krafft, S., Göhmann, H. D., Sommer, J., Straube, A. & Ruscheweyh, R. Learned control over spinal nociception in patients with chronic back pain. *European Journal of Pain (United Kingdom)* **21**, 1538–1549 (2017).
23. Fierro, B. *et al.* Repetitive transcranial magnetic stimulation (rTMS) of the dorsolateral prefrontal cortex (DLPFC) during capsaicin-induced pain: modulatory effects on motor cortex excitability. *Exp Brain Res* **203**, 31–38 (2010).
24. Lorenz, J., Minoshima, S. & Casey, K. L. Keeping pain out of mind: the role of the dorsolateral prefrontal cortex in pain modulation. *Brain* **126**, 1079–1091 (2003).
25. Bogdanov, V. B. *et al.* Cerebral responses and role of the prefrontal cortex in conditioned pain modulation: an fMRI study in healthy subjects. *Behavioural Brain Research* **281**, 187–198 (2015).
26. Bunk, S. *et al.* Pain processing in older adults and its association with prefrontal characteristics. *Brain Sci* **10**, 1–17 (2020).
27. Kanda, M. *et al.* Transcranial magnetic stimulation (TMS) of the sensorimotor cortex and medial frontal cortex modifies human pain perception. *Clinical Neurophysiology* **114**, 860–866 (2003).
28. Alonso-Matielo, H. *et al.* Electrical stimulation of the posterior insula induces mechanical analgesia in a rodent model of neuropathic pain by modulating GABAergic signaling and activity in the pain circuitry. *Brain Res* **1754**, 147237 (2021).
29. Liu, C.-C., Moosa, S., Quigg, M. & Elias, W. J. Anterior insula stimulation increases pain threshold in humans: a pilot study. *J Neurosurg* **135**, 1487–1492 (2021).
30. Kang, S. J. *et al.* Bidirectional modulation of hyperalgesia via the specific control of excitatory and inhibitory neuronal activity in the ACC. *Mol Brain* **8**, 1–11 (2015).
31. Gu, L. *et al.* Pain inhibition by optogenetic activation of specific anterior cingulate cortical neurons. *PLoS One* **10**, 1–17 (2015).
32. Bingel, U. & Tracey, I. Imaging CNS modulation of pain in humans. *Physiology* vol. 23 Preprint at https://doi.org/10.1152/physiol.00024.2008 (2008).
33. Schulz, E., Stankewitz, A., Witkovský, V., Winkler, A. M. & Tracey, I. Strategy-dependent modulation of cortical pain circuits for the attenuation of pain. *Cortex* (2019) doi:10.1016/j.cortex.2018.12.014.
34. Seminowicz, D. A., Mikulis, D. J. & Davis, K. D. Cognitive modulation of pain-related brain responses depends on behavioral strategy. *Pain* **112**, 48–58 (2004).
35. Ruscheweyh, R. *et al.* Control over spinal nociception as quantified by the nociceptive flexor reflex (RIII reflex) can be achieved under feedback of the RIII reflex. *European Journal of Pain (United Kingdom)* **19**, 480–489 (2015).
36. Krafft, S., Göhmann, H. D., Sommer, J., Straube, A. & Ruscheweyh, R. Learned control over spinal nociception in patients with chronic back pain. *European Journal of Pain (United Kingdom)* **21**, 1538–1549 (2017).
37. Bouhassira, D., Danziger, N., Atta, N. & Guirimand, F. Comparison of the pain suppressive effects of clinical and experimental painful conditioning stimuli. *Brain* **126**, 1068–1078 (2003).
38. Willer, J. C. Comparative study of perceived pain and nociceptive flexion reflex in man. *Pain* **3**, 69–80 (1977).
39. Sandrini, G. *et al.* The lower limb flexion reflex in humans. *Prog Neurobiol* **77**, 353–395 (2005).
40. Bates, D., Maechler, M., Bolker, B. & Walker, S. Fitting Linear Mixed-Effects Models Using lme4. *J Stat Softw* **67**, 1–48 (2015).
41. Fox, J. & Weisberg, S. *An {R} Companion to Applied Regression*. (Sage, 2019).
42. Esteban, O. *et al.* fMRIPrep: a robust preprocessing pipeline for functional MRI. *Nat Methods* (2019) doi:10.1038/s41592-018-0235-4.
43. Gorgolewski, K. *et al.* Nipype: A flexible, lightweight and extensible neuroimaging data processing framework in Python. *Front Neuroinform* (2011) doi:10.3389/fninf.2011.00013.
44. Tustison, N. J. *et al.* N4ITK: Improved N3 bias correction. *IEEE Trans Med Imaging* (2010) doi:10.1109/TMI.2010.2046908.
45. Dale, A. M., Fischl, B. & Sereno, M. I. Cortical Surface-Based Analysis. *Neuroimage* **9**, 179–194 (1999).
46. Klein, A. *et al.* Mindboggling morphometry of human brains. *PLoS Comput Biol* (2017) doi:10.1371/journal.pcbi.1005350.

47. Fonov, V., Evans, A., McKinstry, R., Almli, C. & Collins, D. Unbiased nonlinear average age-appropriate brain templates from birth to adulthood. *Neuroimage* (2009) doi:10.1016/s1053-8119(09)70884-5.
48. Avants, B., Tustison, N. & Song, G. Advanced Normalization Tools (ANTS). *Insight Journal* (2009).
49. Zhang, Y., Brady, M. & Smith, S. Segmentation of brain MR images through a hidden Markov random field model and the expectation-maximization algorithm. *IEEE Trans Med Imaging* (2001) doi:10.1109/42.906424.
50. Cox, R. W. AFNI: Software for analysis and visualization of functional magnetic resonance neuroimages. *Computers and Biomedical Research* (1996) doi:10.1006/cbmr.1996.0014.
51. Jenkinson, M., Bannister, P., Brady, M. & Smith, S. Improved optimization for the robust and accurate linear registration and motion correction of brain images. *Neuroimage* (2002) doi:10.1016/S1053-8119(02)91132-8.
52. Greve, D. N. & Fischl, B. Accurate and robust brain image alignment using boundary-based registration. *Neuroimage* (2009) doi:10.1016/j.neuroimage.2009.06.060.
53. Behzadi, Y., Restom, K., Liau, J. & Liu, T. T. A component based noise correction method (CompCor) for BOLD and perfusion based fMRI. *Neuroimage* (2007) doi:10.1016/j.neuroimage.2007.04.042.
54. Power, J. D. *et al.* Methods to detect, characterize, and remove motion artifact in resting state fMRI. *Neuroimage* (2014) doi:10.1016/j.neuroimage.2013.08.048.
55. Pruim, R. H. R. *et al.* ICA-AROMA: A robust ICA-based strategy for removing motion artifacts from fMRI data. *Neuroimage* (2015) doi:10.1016/j.neuroimage.2015.02.064.
56. Murphy, K., Bodurka, J. & Bandettini, P. A. How long to scan? The relationship between fMRI temporal signal to noise and necessary scan duration. *Neuroimage* **34**, 565–574 (2007).
57. Guillaume, B., Hua, X., Thompson, P. M., Waldorp, L. & Nichols, T. E. Fast and accurate modelling of longitudinal and repeated measures neuroimaging data. *Neuroimage* **94**, 287–302 (2014).
58. Guillaume, B. & Nichols, T. E. Non-parametric Inference for Longitudinal and Repeated-Measures Neuroimaging Data with the Wild Bootstrap. *Organization for Human Brain Mapping (OHBM) in Hawaii* Preprint at (2015).
59. Gentili, C., Cecchetti, L., Handjaras, G., Lettieri, G. & Cristea, I. A. The case for preregistering all region of interest (ROI) analyses in neuroimaging research. *Eur J Neurosci* **53**, 357–361 (2021).
60. Meeker, T. J. *et al.* Tonic pain alters functional connectivity of the descending pain modulatory network involving amygdala, periaqueductal gray, parabrachial nucleus and anterior cingulate cortex. *Neuroimage* **256**, (2022).
61. Seminowicz, D. A. & Moayedi, M. The dorsolateral prefrontal cortex in acute and chronic pain. *The journal of pain : official journal of the American Pain Society* **18**, 1027 (2017).
62. Edlow, B. L. *et al.* Neuroanatomic connectivity of the human ascending arousal system critical to consciousness and its disorders. *J Neuropathol Exp Neurol* (2012) doi:10.1097/NEN.0b013e3182588293.
63. Zhou, Y., Shi, L., Cui, X., Wang, S. & Luo, X. Functional connectivity of the caudal anterior cingulate cortex is decreased in autism. *PLoS One* **11**, (2016).
64. Karlsson, K. A. E. *et al.* Modulation of hypothalamus and amygdalar activation levels with stimulus valence. *Neuroimage* **51**, 324–328 (2010).
65. Rolls, E. T., Huang, C. C., Lin, C. P., Feng, J. & Joliot, M. Automated anatomical labelling atlas 3. *Neuroimage* (2020) doi:10.1016/j.neuroimage.2019.116189.
66. Fan, L. *et al.* The Human Brainnetome Atlas: A New Brain Atlas Based on Connectional Architecture. *Cereb Cortex* **26**, 3508–3526 (2016).
67. Lewis, L. D., Setsompop, K., Rosen, B. R. & Polimeni, J. R. Stimulus-dependent hemodynamic response timing across the human subcortical-cortical visual pathway identified through high spatiotemporal resolution 7T fMRI. *Neuroimage* **181**, 279–291 (2018).
68. Bomyea, J. *et al.* Change in neural response during emotion regulation is associated with symptom reduction in cognitive behavioral therapy for anxiety disorders. *Journal of Affective Disorders* vol. 271 Preprint at https://doi.org/10.1016/j.jad.2020.04.001 (2020).
69. Porro, C. A. *et al.* Does anticipation of pain affect cortical nociceptive systems? *J Neurosci* **22**, 3206–3214 (2002).
70. Piché, M., Arsenault, M. & Rainville, P. Cerebral and cerebrospinal processes underlying counterirritation analgesia. *Journal of Neuroscience* **29**, 14236–14246 (2009).

71. Wager, T. D. *et al.* An fMRI-Based Neurologic Signature of Physical Pain. *New England Journal of Medicine* **368**, 1388–1397 (2013).
72. Morton, D.L Sandhu J, S. J. A. K. Brain imaging of pain: state of the art. *J Pain Res* **9**, 613–624 (2016).
73. Bäumler, M. *et al.* Learned control over spinal nociception: Transfer and stability of training success in a long-term study. *Clinical Neurophysiology* **128**, 2462–2469 (2017).
74. Atlas, L. Y. & Wager, T. D. A Meta-analysis of Brain Mechanisms of Placebo Analgesia: Consistent Findings and Unanswered Questions. in *Placebo* (eds. Benedetti, F., Enck, P., Frisaldi, E. & Schedlowski, M.) 37–69 (Springer Berlin Heidelberg, 2014).
75. Wager, T. D. & Fields, H. Placebo analgesia. in *Textbook of Pain* (eds. Kolzenburg, M. & Turk, T.) (Saunders Elsevier, 2013).
76. Hadjipavlou, G., Dunckley, P., Behrens, T. E. & Tracey, I. Determining anatomical connectivities between cortical and brainstem pain processing regions in humans: A diffusion tensor imaging study in healthy controls. *Pain* **123**, 169–178 (2006).
77. Kong, J., Tu, P., Zyloney, C. & Su, T. Intrinsic functional connectivity of the periaqueductal gray, a resting fMRI study. *Behavioural Brain Research* **211**, 215–219 (2010).
78. Mylius, V. *et al.* Effects of transcranial direct current stimulation on pain perception and working memory. *European Journal of Pain (United Kingdom)* **16**, 974–982 (2012).
79. Fierro, B. *et al.* Modulation of pain perception by transcranial magnetic stimulation of left prefrontal cortex. *Journal of Headache and Pain* **12**, 185–191 (2011).
80. Behbehani, M., Park, M. & Clement, M. Interactions between the lateral hypothalamus and the periaqueductal gray. *The Journal of Neuroscience* **8**, 2780–2787 (1988).
81. Gerashchenko, D., Horvath, T. L. & Xie, X. (Simon). Direct inhibition of hypocretin/orexin neurons in the lateral hypothalamus by nociceptin/orphanin FQ blocks stress-induced analgesia in rats. *Neuropharmacology* **60**, 543–549 (2011).
82. Ezzatpanah, S., Babapour, V., Sadeghi, B. & Haghparast, A. Chemical stimulation of the lateral hypothalamus by carbachol attenuated the formalin-induced pain behaviors in rats. *Pharmacol Biochem Behav* **129**, 105–110 (2015).
83. Ploner, M., Lee, M. C., Wiech, K., Bingel, U. & Tracey, I. Prestimulus functional connectivity determines pain perception in humans. *Proc Natl Acad Sci U S A* **107**, 355–360 (2010).
84. Geuter, S., Boll, S., Eippert, F. & Büchel, C. Functional dissociation of stimulus intensity encoding and predictive coding of pain in the insula. *Elife* **6**, 1–22 (2017).
85. Wiech, K. *et al.* Anterior Insula Integrates Information about Salience into Perceptual Decisions about Pain. *Journal of Neuroscience* **30**, 16324–16331 (2010).
86. Brown, C. A. & Jones, A. K. A role for midcingulate cortex in the interruptive effects of pain anticipation on attention. *Clin Neurophysiol* **119**, 2370–2379 (2008).
87. Casey, K. L., Morrow, T. J., Lorenz, J. & Minoshima, S. Temporal and spatial dynamics of human forebrain activity during heat pain: Analysis by positron emission tomography. *J Neurophysiol* **85**, 951–959 (2001).
88. Ploghaus, A. *et al.* Dissociating pain from its anticipation in the human brain. *Science (1979)* **284**, 1979–1981 (1999).
89. Palermo, S., Benedetti, F., Costa, T. & Amanzio, M. Pain anticipation: an activation likelihood estimation meta-analysis of brain imaging studies. *Hum Brain Mapp* **36**, 1648–1661 (2015).
90. Segerdahl, A. R., Mezue, M., Okell, T. W., Farrar, J. T. & Tracey, I. The dorsal posterior insula subserves a fundamental role in human pain. *Nat Neurosci* **18**, 499–500 (2015).
91. Lu, C. *et al.* Insular Cortex is Critical for the Perception, Modulation, and Chronification of Pain. *Neurosci Bull* **32**, 191–201 (2016).
92. Nir, R.-R. *et al.* Neurophysiology of the Cortical Pain Network: Revisiting the Role of S1 in Subjective Pain Perception Via Standardized Low-Resolution Brain Electromagnetic Tomography (sLORETA). *J Pain* **9**, 1058–1069 (2008).
93. Oshiro, Y., Quevedo, A. S., McHaffie, J. G., Kraft, R. A. & Coghill, R. C. Brain mechanisms supporting discrimination of sensory features of pain: A new model. *Journal of Neuroscience* **29**, 14924–14931 (2009).
94. Osborne, P. B., Vaughan, C. W., Wilson, H. I. & Christie, M. J. Opioid inhibition of rat periaqueductal grey neurones with identified projections to rostral ventromedial medulla in vitro. *Journal of Physiology* **490**, 383–389 (1996).

95. Rhodes, D. L. & Liebeskind, J. C. Analgesia from rostral brain stem stimulation in the rat. *Brain Res* **143**, 521–532 (1978).
96. Fields, H. L., Wagner, G. M. & Anderson, S. D. Some properties of spinal neurons projecting to the medial brain-stem reticular formation. *Exp Neurol* **47**, 118–134 (1975).
97. Smith, D. J. *et al.* The μ opiate receptor is responsible for descending pain inhibition originating in the periaqueductal gray region of the rat brain. *Eur J Pharmacol* **156**, 47–54 (1988).
98. Zhuo, M. & Gebhart, G. F. Biphasic Modulation of Spinal Nociceptive Transmission From the Medullary Raphe Nuclei in the Rat. *J Neurophysiol* **78**, 746–758 (1997).
99. Margalit, D. & Segal, M. A pharmacologic study of analgesia produced by stimulation of the nucleus locus coeruleus. *Psychopharmacology (Berl)* **62**, 169–173 (1979).
100. Fields, H., Bry, J., Hentall, I. & Zorman, G. The activity of neurons in the rostral medulla of the rat during withdrawal from noxious heat. *The Journal of Neuroscience* **3**, 2545–2552 (1983).
101. Hosobuchi, Y., Adams, J. E. & Linchitz, R. Pain relief by electrical stimulation of the central gray matter in humans and its reversal by naloxone. *Science (1979)* **197**, 183–186 (1977).
102. Hosobuchi, Y. Dorsal Periaqueductal Gray-Matter Stimulation in Humans. *Pacing and Clinical Electrophysiology* **10**, 213–216 (1987).
103. Young, R. F. & Chambi, V. I. Pain relief by electrical stimulation of the periaqueductal and periventricular gray matter. *J Neurosurg* **66**, 364–371 (1987).
104. Wager, T. D. *et al.* Placebo-Induced Changes in fMRI in the Anticipation and Experience of Pain. *Science (1979)* **303**, 1162–1167 (2004).
105. Greenspan, J. D. & Winfield, J. A. Reversible pain and tactile deficits associated with a cerebral tumor compressing the posterior insula and parietal operculum. *Pain* **50**, 29–39 (1992).
106. Cerliani, L. *et al.* Probabilistic tractography recovers a rostrocaudal trajectory of connectivity variability in the human insular cortex. *Hum Brain Mapp* **33**, 2005–2034 (2012).
107. Seminowicz, D. A. & Moayedi, M. The Dorsolateral Prefrontal Cortex in Acute and Chronic Pain. *J Pain* **18**, 1027–1035 (2017).
108. Wager, T. D. *et al.* Placebo-Induced Changes in fMRI in the Anticipation and Experience of Pain. *Science (1979)* **303**, 1162–1167 (2004).
109. Lorenz, J., Minoshima, S. & Casey, K. L. Keeping pain out of mind: the role of the dorsolateral prefrontal cortex in pain modulation. *Brain* **126**, 1079–1091 (2003).
110. Mantyh, P. W. Connections of midbrain periaqueductal gray in the monkey. I. Ascending efferent projections. *J Neurophysiol* **49**, 567–581 (1983).
111. Bannister, K. & Dickenson, A. H. What do monoamines do in pain modulation? *Curr Opin Support Palliat Care* **10**, 143–148 (2016).
112. Kwon, M., Altin, M., Duenas, H. & Alev, L. The Role of Descending Inhibitory Pathways on Chronic Pain Modulation and Clinical Implications. *Pain Practice* **14**, 656–667 (2014).
113. Xie, Y. F., Huo, F. Q. & Tang, J. S. Cerebral cortex modulation of pain. *Acta Pharmacologica Sinica 2009 30:1* **30**, 31–41 (2008).
114. Cervenka, S. *et al.* Changes in dopamine D2-receptor binding are associated to symptom reduction after psychotherapy in social anxiety disorder. *Transl Psychiatry* **2**, (2012).
115. Pfeifer, P. *et al.* Prefrontal and striatal dopamine D2/D3 receptors correlate with fMRI BOLD activation during stopping. *Brain Imaging Behav* **16**, 186–198 (2022).
116. Serafini, R. A., Pryce, K. D. & Zachariou, V. The Mesolimbic Dopamine System in Chronic Pain and Associated Affective Comorbidities. *Biol Psychiatry* **87**, 64 (2020).
117. Oliva, V., Hartley-Davies, R., Moran, R., Pickering, A. E. & Brooks, J. C. W. Simultaneous Brain, Brainstem and Spinal Cord pharmacological-fMRI reveals involvement of an endogenous opioid network in attentional analgesia. *Elife* **11**, (2022).
118. Karjalainen, T. *et al.* Dissociable Roles of Cerebral μ-Opioid and Type 2 Dopamine Receptors in Vicarious Pain: A Combined PET–fMRI Study. *Cerebral Cortex* **27**, 4257–4266 (2017).
119. Thompson, S. J. *et al.* Chronic neuropathic pain reduces opioid receptor availability with associated anhedonia in rat. *Pain* **159**, 1856 (2018).
120. Khan, H. S. & Stroman, P. W. Inter-individual differences in pain processing investigated by functional magnetic resonance imaging of the brainstem and spinal cord. *Neuroscience* **307**, 231–241 (2015).

121. Coghill, R. C., McHaffie, J. G. & Yen, Y. F. Neural correlates of interindividual differences in the subjective experience of pain. *Proc Natl Acad Sci U S A* **100**, 8538–8542 (2003).
122. Graeff, P., Itter, A., Wach, K. & Ruscheweyh, R. Inter-individual differences explain more variance in conditioned pain modulation than age, sex and conditioning stimulus intensity combined. *Brain Sci* **11**, (2021).
123. Yarnitsky, D. *et al.* Prediction of chronic post-operative pain: Pre-operative DNIC testing identifies patients at risk. *Pain* **138**, 22–28 (2008).
124. Rypma, B., Berger, J. S., Genova, H. M., Rebbechi, D. & Esposito, M. D. DISSOCIATING AGE-RELATED CHANGES IN COGNITIVE STRATEGY AND NEURAL EFFICIENCY USING EVENT- RELATED fMRI. *Response* **3**, (2002).
125. Lutz, J. *et al.* Mindfulness and emotion regulation-an fMRI study. *Soc Cogn Affect Neurosci* **9**, 776–785 (2013).
126. Ives-Deliperi, V. L., Solms, M. & Meintjes, E. M. The neural substrates of mindfulness: An fMRI investigation. *Soc Neurosci* **6**, 231–242 (2011).
127. Boccia, M. *et al.* A penny for your thoughts! patterns of fMRI activity reveal the content and the spatial topography of visual mental images. *Hum Brain Mapp* **36**, 945–958 (2015).
128. Edwards, R. R. Individual differences in endogenous pain modulation as a risk factor for chronic pain. *Neurology* **65**, 437–443 (2005).
129. Lee, J. W. & Yoon, S. W. Effects of measurement posture and stimulation intensity on the nociceptive flexion reflex (RIII reflex). *J Phys Ther Sci* **29**, 1066–1069 (2017).
130. Liu, J. Z., Zhang, L., Brown, R. W. & Yue, G. H. Reproducibility of fMRI at 1.5 T in a strictly controlled motor task. *Magn Reson Med* **52**, 751–760 (2004).


**Data and Code Availability Statement:** Defaced data in BIDS format will be made publicly available upon acceptance on https://gin.g-node.org/

**Credit Author Statement**

**Philipp Graeff**: Methodology, Software, Formal analysis, Investigation, Data Curation, Writing - Original Draft, Visualization. **Ruth Ruscheweyh**: Conceptualization, Methodology, Validation, Writing – Review & Editing, Supervision, Project administration, Funding acquisition. **Virginia L. Flanagin**: Conceptualization, Methodology, Validation, Writing – Review & Editing, Visualization, Supervision, Project administration, Funding acquisition.

Declaration of Interest Statement: none